Supporting Information:

Cesium Power: Low Cs^+ Levels Impart Stability to Perovskite Solar Cells

Melepurath Deepa,[a#] Manuel Salado,[b#] Laura Calio[b], Samrana Kazim[b], S. M. Shivaprasad[c] and Shahzada Ahmad[b]

[a]Department of Chemistry, Indian Institute of Technology Hyderabad, Kandi-502285, Sangareddy, Telangana (India)

[b]Abengoa Research, Abengoa, C/ Energía Solar no 1, Campus Palmas, Altas, 41014, Sevilla, Spain

[c]International Centre for Materials Science, Chemistry and Physics of Materials Unit, Jawaharlal Nehru Centre for Advanced Scientific Research, Jakkur, Bangalore. 560064 (India)

Email: shahzada.ahmad@abengoa.com

Table S1: Statistical data for solar cell parameters of the $(MA_{0.15}FA_{0.85})Pb(I_{0.85}Br_{0.15})_3$ cells with perovskites without and with Cs^+.

Sample	V_{OC} (V)	J_{SC} (mA cm^{-2})	FF	η (%)
0%	0.9999 ± 0.0226	21.0195 ± 0.2954	68.5020 ± 5.0153	14.4264 ± 1.2599
5%	1.0195 ± 0.0427	21.25626 ± 0.5689	73.91142 ± 1.0073	16.03272 ± 1.0937
10%	1.0409 ± 0.0273	20.1513 ± 1.9052	67.1781 ± 1.7671	14.0892 ± 1.4132

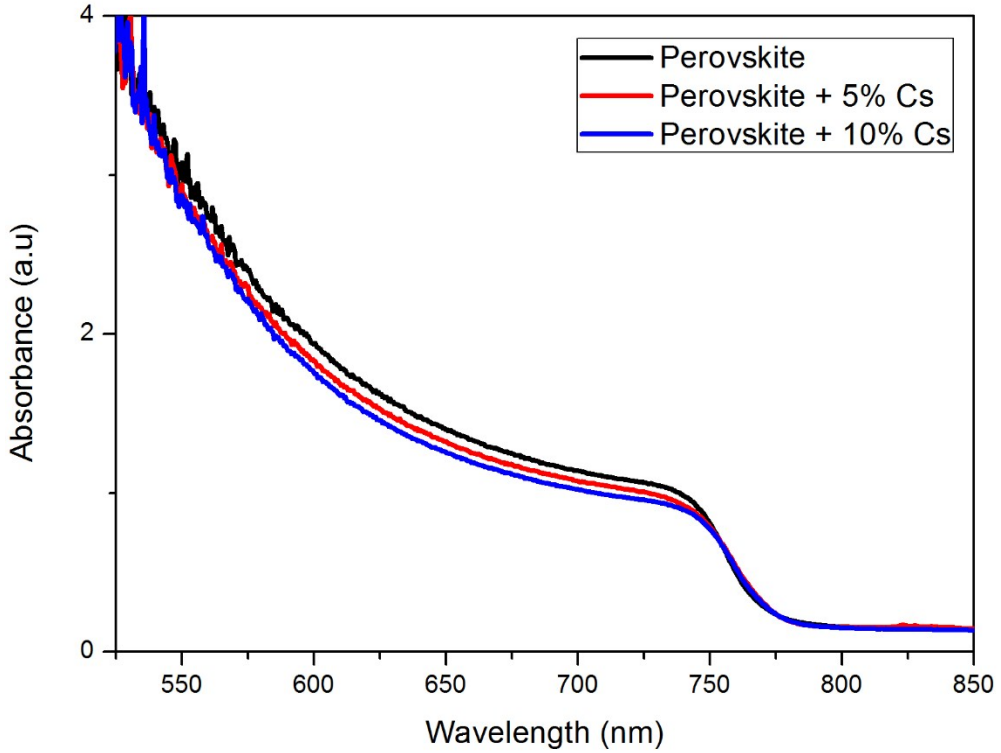

Fig. S1: Absorption spectra of $(MA_{0.15}FA_{0.85})Pb(I_{0.85}Br_{0.15})_3$, $Cs_{0.05}(MA_{0.15}FA_{0.85})_{0.95}Pb(I_{0.85}Br_{0.15})_3$, and $Cs_{0.1}(MA_{0.15}FA_{0.85})_{0.9}Pb(I_{0.85}Br_{0.15})_3$ perovskites.

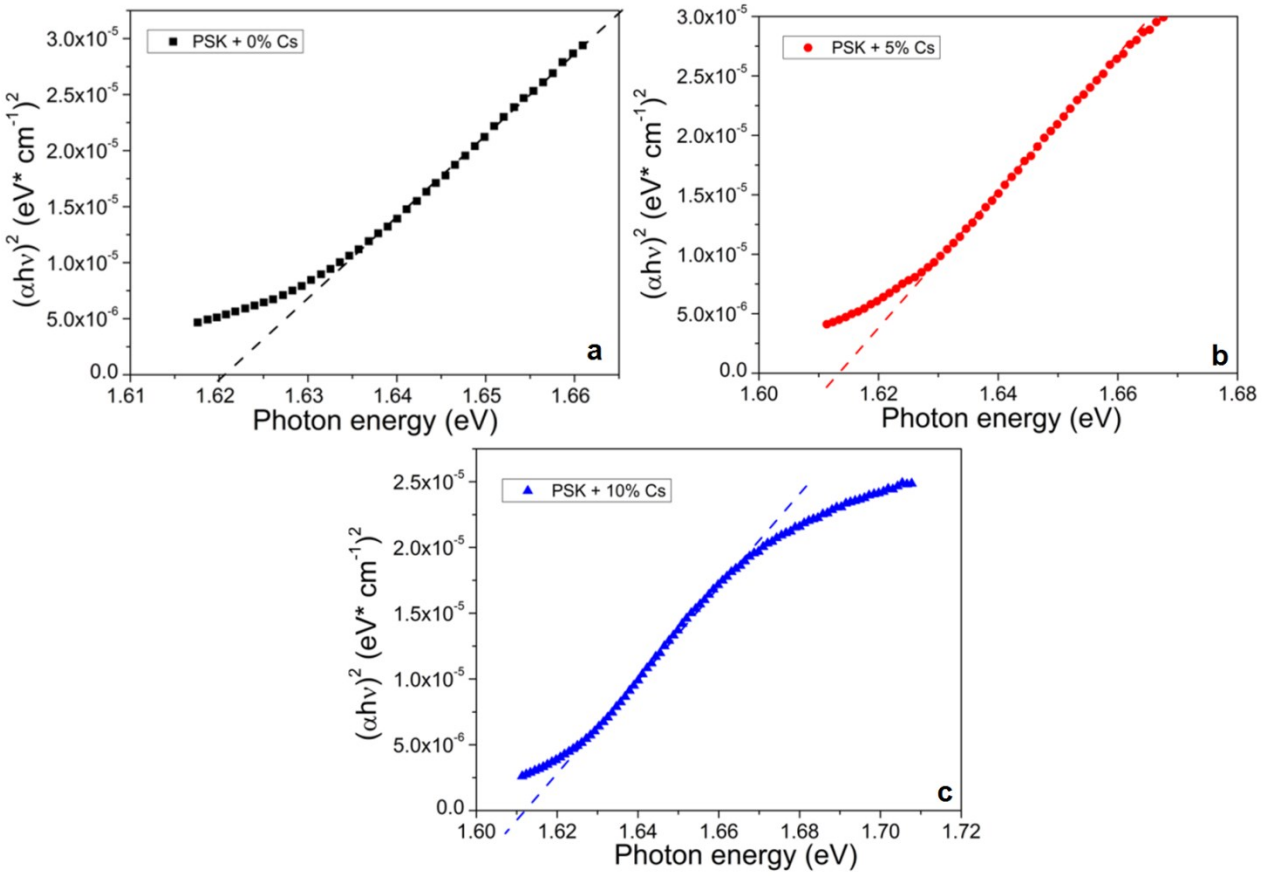

Fig. S2: Tauc plots of (a) $(MA_{0.15}FA_{0.85})Pb(I_{0.85}Br_{0.15})_3$, (b) $Cs_{0.05}(MA_{0.15}FA_{0.85})_{0.95}Pb(I_{0.85}Br_{0.15})_3$ and (c) $Cs_{0.1}(MA_{0.15}FA_{0.85})_{0.9}Pb(I_{0.85}Br_{0.15})_3$ perovskites.

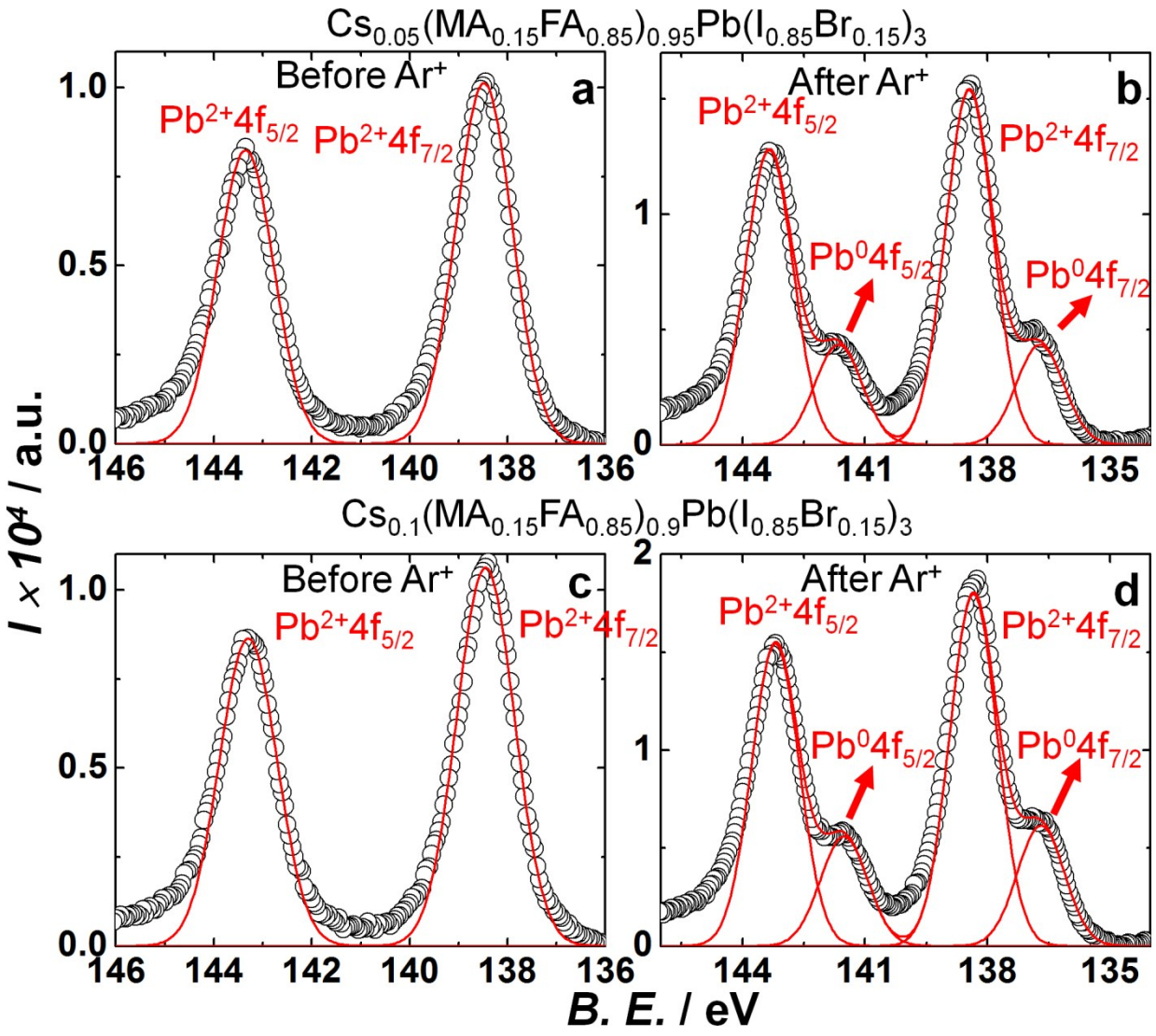

Fig. S3: Deconvoluted core level spectra of Pb4f: (a,c) before and (b,d,) after Ar^+ sputter for the perovskites with Cs^+.

Table S2: Assignments corresponding to the deconvoluted core level and valence band spectra of perovskite electrodes. MA and FA are CH_3NH_3 and $HC(NH_2)_2$ respectively and the proportion of Cs^+ is in x/100 (%). FWHM is full width at half maximum.

Component	$(MA_{0.15}FA_{0.85})Pb(I_{0.85}Br_{0.15})_3$		$Cs_{0.05}(MA_{0.15}FA_{0.85})_{0.95}Pb(I_{0.85}Br_{0.15})_3$		$Cs_{0.1}(MA_{0.15}FA_{0.85})_{0.9}Pb(I_{0.85}Br_{0.15})_3$	
	BE (eV)		BE (eV)		BE (eV)	
	Before Ar+ sputter	After Ar+ sputter	Before Ar+ sputter	After Ar+ sputter	Before Ar+ sputter	After Ar+ sputter
$Pb^{2+}4f_{7/2}$	138.5	138.3	138.5	138.3	138.5	138.34
	(55.37)	(39.53)	(55.14)	(41.76)	(55.19)	(39.79)
FWHM	1.374	1.391	1.35	1.373	1.384	1.364
$Pb^{2+}4f_{5/2}$	143.3	143.2	143.35	143.2	143.3	143.2
	(45.68)	(33.48)	(44.85)	(34.67)	(44.80)	(34.22)
FWHM	1.374	1.391	1.35	1.373	1.384	1.364
$Pb^{0}4f_{7/2}$	---	136.7	---	136.7	---	136.7
		(13.95)		(11.78		(13.61)
FWHM		1.391		1.373		1.364
$Pb^{0}4f_{5/2}$	---	141.49	---	141.65	---	141.51
		(13.02)		(11.78)		(12.36)
FWHM		1.391		1.373		1.364
$Pb^{2+}4d_{5/2}$	413.7	413.35	413.9	413.55	413.8	413.4
FWHM	3.87	4.89	4.2	4.53	4.38	4.63
Br3d	68.5	68.44	68.7	68.4	68.6	68.4
$Cs3d_{5/2}$	---	---	724.7	724.6	724.86	725.09
			(41.07)	(44.05)	(14.5)	(18.18)
FWHM			2.03	1.88	3.05	1.77
$Cs3d_{3/2}$	---	---	738.7	738.6	738.40	739.22
			(23.85)	(36.22)	(4.84)	(16.39)
FWHM			1.75	2.16	1.59	2.08
Cs	---	---	716.5	717.05	716.57	717.02
			(35.07)	(19.73)	(80.64)	(65.41)
FWHM			3.68	3.96	4.16	3.15
C1s	284.6	284.6	284.6	284.6	284.6	284.6
	(69.01)	(63.31)	(68.31)	(69.66)	(49.71)	(65.74)
FWHM	2.11	2.17	2.13	2.3	2.06	2.12
C1s	287.13	287.75	287.9	288.17	287.6	287.8
	(31)	(36.69)	(31.7)	(30.33)	(50.28)	(34.26)
FWHM	2.11	2.17	2.13	2.3	2.06	2.12
N1s	400.7	400.7	400.76	401.02	400.8	400.9
FWHM	1.47	2.17	1.49	3.05	1.54	2.94
$I3d_{5/2}$	619.4	619.35	619.53	619.5	619.5	619.53
	(58.71)	(57.5)	(58)	(58)	(57.7)	(58.83)
FWHM	1.6	1.66	1.63	1.61	1.62	1.62
$I3d_{3/2}$	631	630.85	631.1	631	631	631
	(41.7)	(42.5)	(42)	(42)	(42.3)	(42.16)
FWHM	1.6	1.66	1.63	1.61	1.62	1.62
$Pb5d_{5/2}$	19.56	19.5	19.5	19.5	19.5	19.5
$Pb5d_{3/2}$	22.19	22.1	22.3	22.3	22.3	22
O1s	532.9	530.6	531.7	530.9	532.15	530.7

The first entry in each box is the peak position. The entries in the brackets are the integrated areas under the peaks in %.

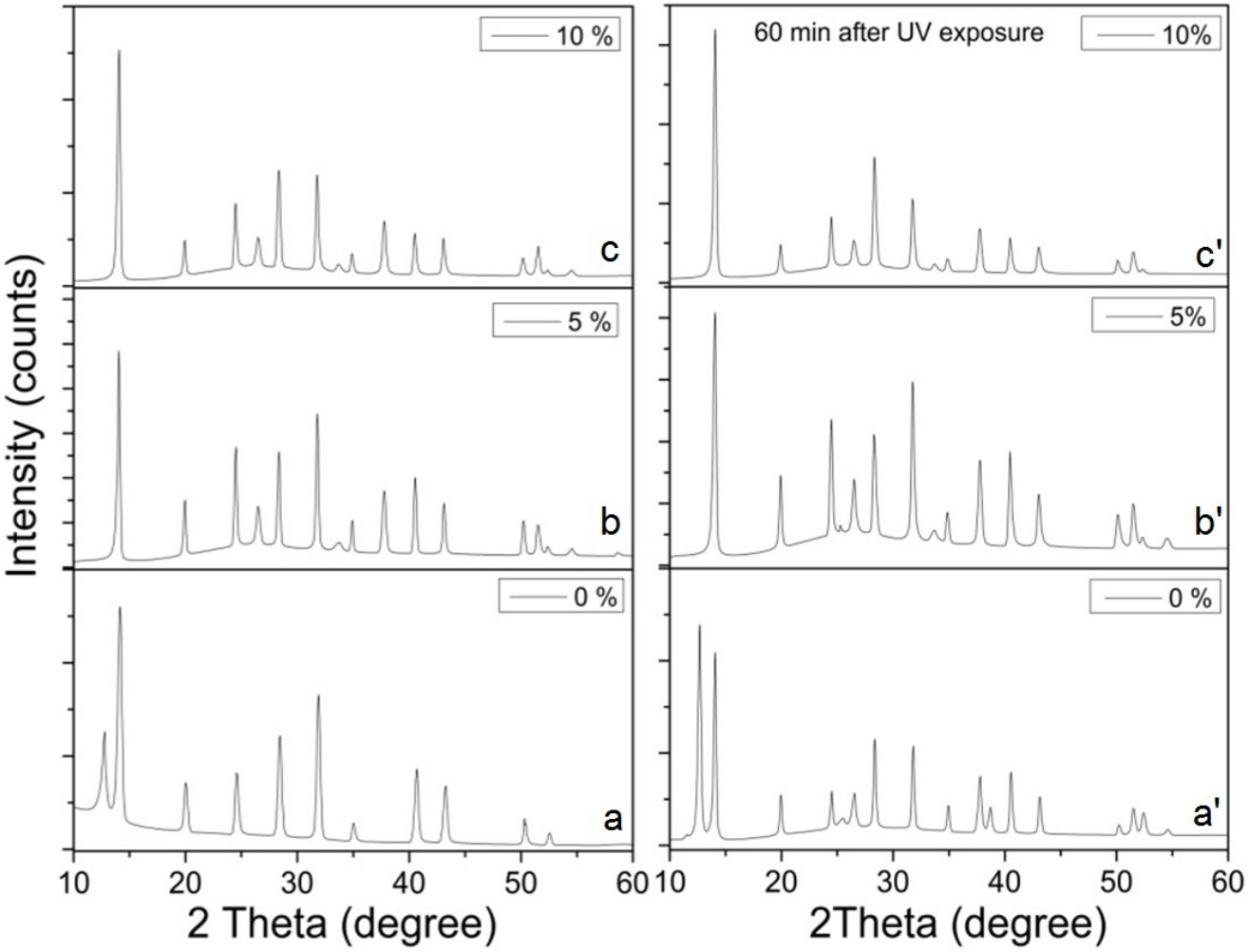

Fig. S4: X-ray diffraction patterns of $(MA_{0.15}FA_{0.85})Pb(I_{0.85}Br_{0.15})_3$, without and with 5 and 10% Cs^+: (a-c) before and (a′-c′) after UV irradiance for 60 min.

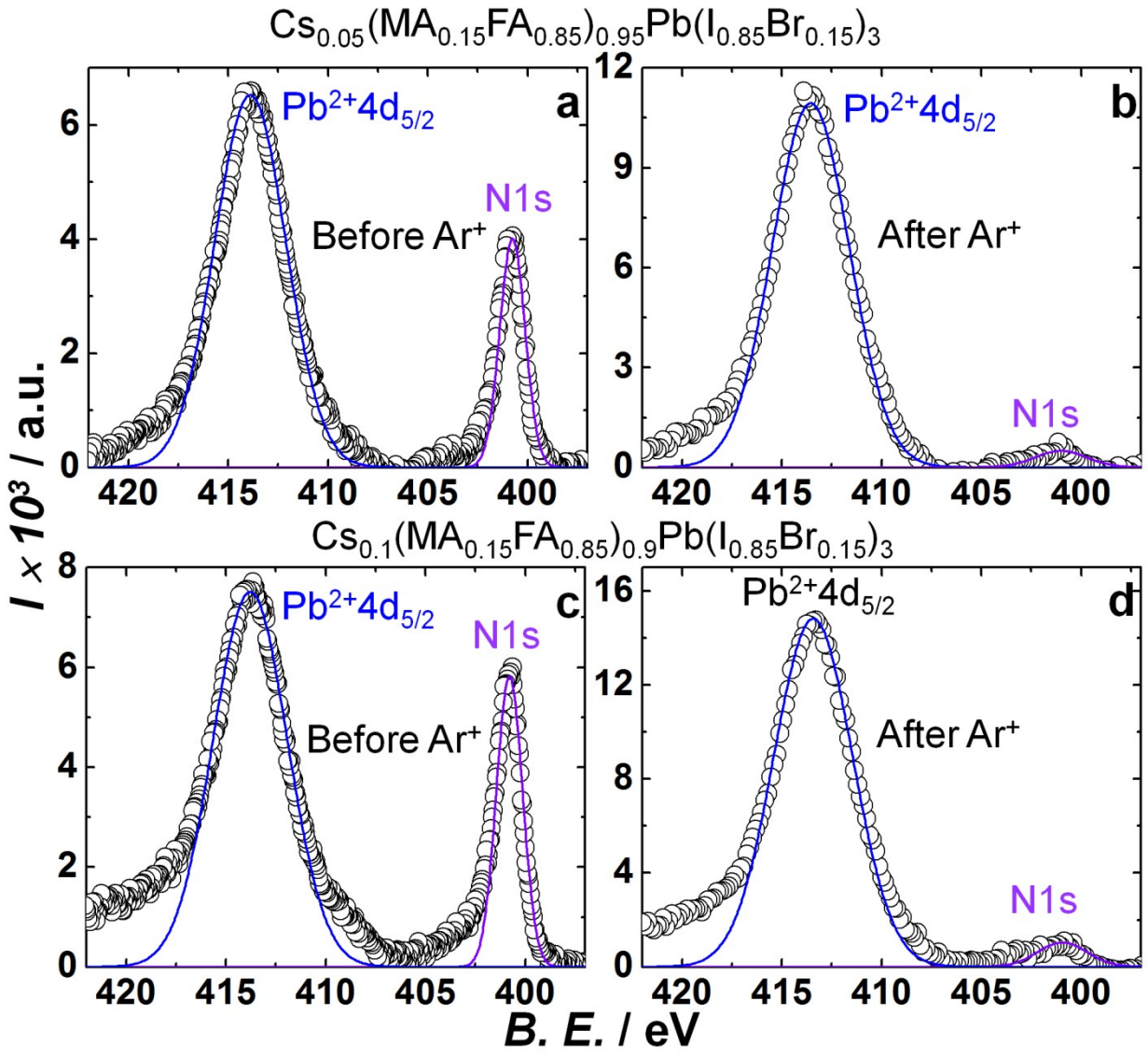

Fig. S5: Deconvoluted core level spectra of Pb4d and N1s: (a,c) before and (b,d,) after Ar^+ sputter for the perovskites with Cs^+.

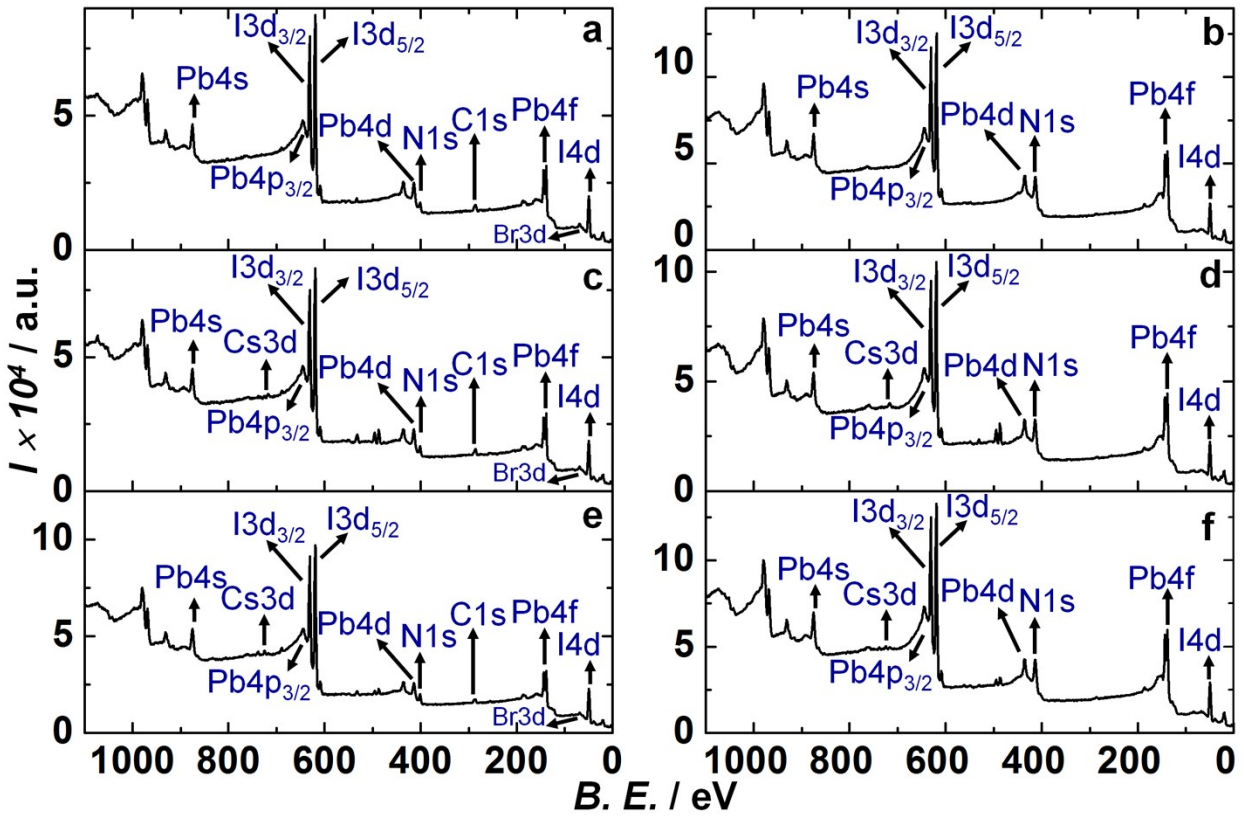

Fig. S6: Survey spectra of (a) before and (b) after Ar^+ sputter for $(MA_{0.15}FA_{0.85})Pb(I_{0.85}Br_{0.15})_3$, (c) before and (d) after Ar^+ sputter for $Cs_{0.05}(MA_{0.15}FA_{0.85})_{0.95}Pb(I_{0.85}Br_{0.15})_3$ and (e) before and (f) after Ar^+ sputter for $Cs_{0.1}(MA_{0.15}FA_{0.85})_{0.9}Pb(I_{0.85}Br_{0.15})_3$.

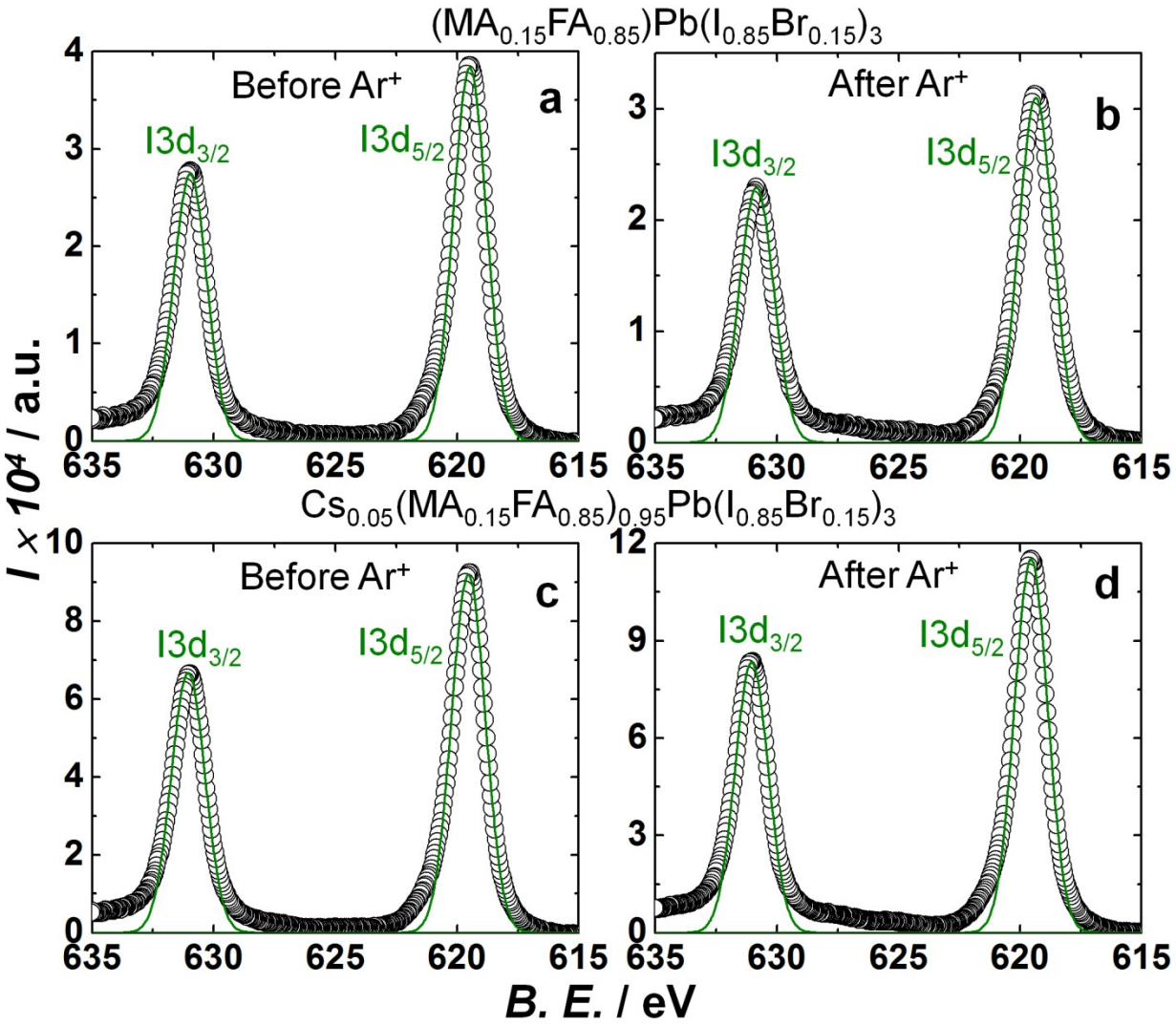

Fig. S7: Deconvoluted core level spectra of I3d: (a) before and (b) after Ar^+ sputter for$(MA_{0.15}FA_{0.85})Pb(I_{0.85}Br_{0.15})_3$, (c) before and (d) after Ar^+ sputter for $Cs_{0.05}(MA_{0.15}FA_{0.85})_{0.95}Pb(I_{0.85}Br_{0.15})_3$.

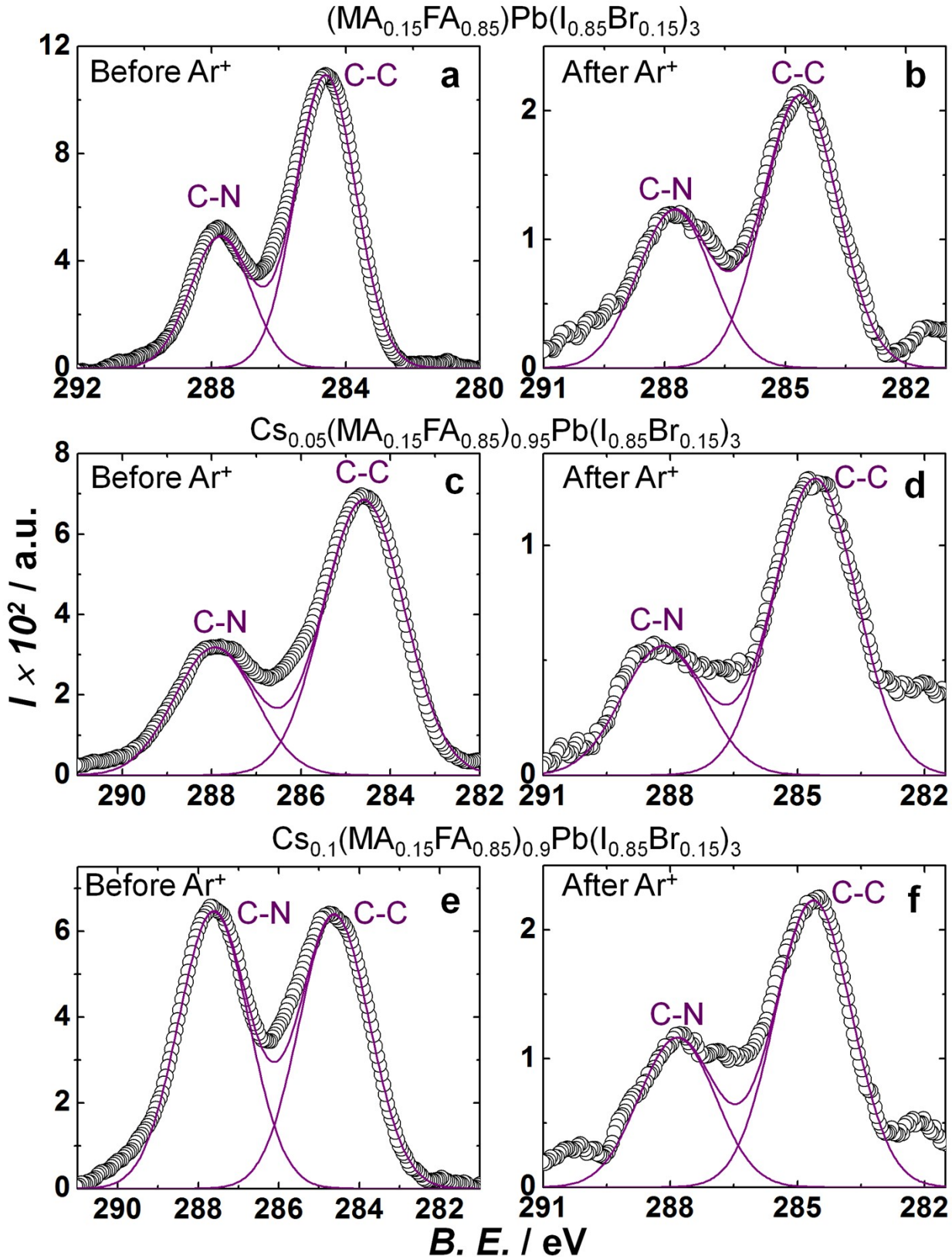

Fig. S8: Deconvoluted core level spectra of C1s: (a,c,e) before and (b,d,f) after Ar^+ sputter for the perovskites with Cs^+.